

**Investigation of electronic structure for  $\beta$ -Zr in the(s-d) subshell**

Abdulhadi Mirdan Ghaleb

Department of physics , College of Science , University of Kirkuk , Kirkuk , Iraq

E-mail : [abdlhadik@yahoo.com](mailto:abdlhadik@yahoo.com)**Abstract**

In this paper, a theoretical study of calculating Compton profiles (CPs) for  $\beta$ -Zr using the renormalized-free-atom model and free electron model for different configurations ( $4d^{3-x}-5s^{1+x}$ ), where ( $x=0.1$  to  $1$  step  $0.1$ ) is presented. The theoretical results and previously experimental data show good agreement and the best electronic configuration found was ( $4d^{2.8}-5s^{1.2}$ ). The cohesive energy of  $\beta$ -Zr is computed by using theoretical Compton profile data and compared with available data. The band structure and density of state of ( $\beta$ -Zr and  $\alpha$ -Zr) phases are determined from density functional theory (DFT) with use Quantum wise Atomistix Tool Kit (ATK), Virtual Nano Lab calculations within the framework of the local density approximation (LDA).

**Keywords:** Compton profile, RFA model, (ATK) simulation package, Cohesive energy.

**1. Introduction**

Zirconium belongs to the 2<sup>nd</sup> series of transition metals, mainly used as a refractory and opactifier, it is used in small amounts as an alloying agent for its strong resistance to corrosion[1]. The electronic band structures of this element are sophisticated and minimal fully grasp in comparison to their cubic counterparts. Despite difficulties due to uniaxial symmetry and two atoms in the unit cell, particular calculations have been reported for zirconium [2-7]. The momentum space counterpart of the electron density, the electron momentum density (EMD),  $n(p)$ , can be similarly used to study chemical bonding. Whereas the electron density ED is higher along covalent bonds, the EMD oscillates along the bonding direction (in reciprocal space). A fitting procedure for extracting EMD properties from the ED has been recently suggested[8]. There are many studies on Compton profile and the electron momentum densities of cubic as well as hcp 3d transition metals have been reported within the last decades[9-11]. The Augment plane wave (APW) band structure determination of the electron momentum distributions and Compton profile in Zr and ZrH<sub>2</sub>, were reported [12]. While, the measurement on this samples were computed using <sup>241</sup>Am  $\gamma$ -ray source[13]. The atomic, binding and electronic structure of very thin Zr chains are studied by the first principle density functional method[14]. The theory of Compton scattering has emerged as a powerful tool for the investigation of the behaviour of valence electrons. Assuming that the impulse approximation holds, the double differential cross section, which measures the amount of photons scattered by the sample into the solid angle  $d\Omega$  with energy  $E_2$ , can be written as[15].

$$\frac{d^2\sigma}{d\Omega dE_2} = C(E_1, E_2, \varphi) J(p_z) \quad (1)$$

Here  $E_1$  is the energy of the incoming photon, ( $\varphi$ ) the scattering angle and  $C(E_1, E_2, \varphi)$  only depends on the setup of the experiment.  $p_z$  is the projection of the initial momentum of the electron onto the scattering vector after collision. The function  $J(p_z)$  is the Compton profile (CP).

$$J(p_z) = \int_{-\infty}^{+\infty} n(p_x, p_y, p_z) dp_x dp_y \quad (2)$$

which measures the projection of the EMD along the direction of the scattering vector  $p_z$  [15]. In all these studies the electron momentum,  $p_z$  is expressed in atomic units (a.u.) where  $e = \hbar = m = 1$ ,  $c = 137$  and 1 a.u. of momentum =  $1.993 \times 10^{-24}$  kg . m/s. In § (2) we present the details of theoretical calculation and, In §(3) and (4) describe the results discussion and conclusions. The aim of present work is the calculation of Compton profiles, band structure and density of state for  $\beta$ -Zr and comparing these with other results of  $\alpha$ -Zr.

**2. Theory****I) Compton profiles :****a) Renormalized – Free-Atom model:**

In the (RFA) model one starts with the free-atom wave function, truncates them at the Wigner-sites (WS) Sphere and renormalizes the wave function to one within this sphere to preserve charge neutrality[16].

For bcc metals, the Compton profile for 5s electrons, can be written as [17]:

$$J_{5s}(P_z) = 4\pi \sum_{n=0}^{\infty} |\Psi_0^c(K_n)|^2 G_n(p_z) \quad (3)$$

Where  $K_n$  is a reciprocal lattice vector and  $p_z$  the projection of electron momentum along the scattering vector direction.  $\Psi_0^c(K_n)$  is the Fourier transform of the RFA wave function  $\phi_0^c(r)$ .

**b) Free Electron model :**

In case of an isotropic momentum distribution, eq. (2) reduces to the well-known form:

$$J_{4s}(p_z) = 2\pi \int_{p_z}^{\infty} dp \rho(\vec{p}) p \quad (4)$$

If we consider the valence electrons in a metal as a non-interacting electron gas, then the momentum density is given by:

$$\rho(\vec{p}) = \text{constant} = \frac{n}{\frac{4}{3}\pi p_F^3} \quad (5)$$

Where  $n$  is the number of free electrons per site and  $p_F$  is the Fermi momentum.

Substitution of  $\rho(p)$  from eq.(5) into eq.(4) gives

$$J_{4s}(p_z) = \frac{3n}{4p_F^3} (p_F^2 - p_z^2) \text{ for } p_z \leq p_F \quad (6)$$

Then free electron gas Compton profile is an inverted parabola including discontinuities of the first derivative at  $\pm p_F$  [18]. From eq.(6), calculated Compton profiles for 5s electron of  $\beta$ -Zr have been done using free electron model.

To get a total profile in the momentum range 0 to +7 a.u., the Compton profile for core electrons were directly taken from the tables of Biggs et al [19].

## II) Cohesive energy:

The cohesive energy which is defined as the difference between the total ground –state energy of the solid and the energy of the individual isolated atoms can be calculated from Compton profile data [20] using the following relation:

$$E_{\text{Coh}} = \int_0^{p_{\text{max}}} p_z^2 [J_s(p_z) - J_{\text{FA}}(p_z)] dp_z \quad (7)$$

Where the  $J_s(p_z)$  and  $J_{\text{FA}}(p_z)$  refer to solid state and free atom profiles, respectively. In this calculation  $p_{\text{max}}$  was taken as infinite. The values of  $J_s(p_z)$  were taken from the RFA calculation which represents the solid-state phase of ( $\beta$ -Zr) and those for free atom Compton profile as shown in table (1). the contributions from the core electrons are same in the  $J_s(p_z)$  and  $J_{\text{FA}}(p_z)$  and hence cancel out in the difference seen in eq.(7) .

## III) Density Functional Theory:

Density functional theory (DFT) is a quantum mechanical modeling used to study the electronic structure of many body system. The properties of many electrons system can be determined by using functional (function of another function). In DFT the functional is the spatially dependent electron density. In DFT, for periodic system, if we can find the electronic states then we can calculate thermal, optical and magnetic properties of solids, equations of state, electron density distributions and cohesive energies [21].

In LDA the functional depends only upon the density at the co-ordinates, where functional is evaluated. This approximation is used to find Eigen function and Eigenvalues of the Hamiltonian. It is commonly used along with plane wave basis. LDA is meant a functional whose functional derivative with respect to density at that point only. It is an approximation to the exchange part which depends upon the value of electron density at each point. This approximation is derived from the homogeneous electron gas model (like Jellium model). We are taking electrons of negative charge around that positive charges are there. So to decrease the interactions between electrons we are considering ex-change term. The exchange functional can also be expressed as the energy of interaction between the electron density and the Fermi Coulomb hole charge distribution. Local Density Approximation is an efficient method for large molecules and solids. In practice, total energy calculations require approximations to be

made for the exchange-correlation energy and Kohn and Sham showed that (LDA) can be written as [22].

$$E_{xc}(n) = \int E_{xc}[n]\rho(r) d^3r \quad (8)$$

where  $\rho$  is the electronic density and ( $E_{xc}[n]$ ) is the exchange-correlation energy per particle of a homogeneous electron gas of charge density  $\rho$ .

$$E_{xc}[n] = E_{xc}(n(r)) \quad (9)$$

LDA exchange correlation potential

$$V_{xc}(r) = \frac{\delta E_{xc}(r)}{\delta n} \quad (10)$$

## IV ) Quantum wise simulation :

ATK is a library of atomic scale modeling techniques that can be used to calculate a wide range of properties of Nano scale systems .New methods are constantly being added to the toolkit, and for each new release ATK will be able to calculate more properties using a wider range of different modeling techniques .The most unique feature is the ability to calculate the electrical properties of nano scale devices ,which consist of a scattering region coupled to two macroscopic bulk system or electrodes [23].

## 3. Results and Discussion

### a) Compton profiles:

The theoretical results of Compton profiles are shown in table (1) in terms of the  $J(0)$  values for the  $\beta$ -Zr metals for different atomic configurations ( $4d^3-5s^1, 4d^{2.9}-5s^{1.1}, 4d^{2.8}-5s^{1.2}, 4d^{2.7}-5s^{1.3}$ ) using renormalized - free-atom model .In the same table also included the theoretical profiles determination by using free electron and free atom models. All results are compared with experimental data [24]. All the theoretical values given in the table (1) are obtained after convoluting the theory with the residual instrumental function (RIF) of 0.6 a.u. and normalized to an area of 16.60175 being the number of electrons from 0 to 7 a.u. In the high momentum region ( $p_z > 3.0$  a.u.), it is seen that all theoretical values are nearly equal. This is easily understood because in this region only core electron contribute in the calculation and for then the same model has been used in all cases. It is interesting to note that values are close to the experiment. At the low momentum region ( $p_z = 0-0.5$  a.u. ), it is seen that the free atom model shows the maximum disagreement. On the whole the RFA values are considerably flatter but the free electron values are close to the experiment. Fig. (1) shows this comparison where we plot the theoretical (except free atom) and experimental results upto 7 a.u. [24]. When ( $p_z > 0.5$  a.u.) it is seen that the RFA values for ( $4d^{2.7}-5s^{1.3}$ ) are lower than ( $4d^3-5s^1, 4d^{2.9}-5s^{1.1}, 4d^{2.8}-5s^{1.2}$ ) results but between ( $p_z > 0.8$  a.u.) a.u. the trend is reversed and the ( $4d^{2.7}-5s^{1.3}$ ) values are higher than from ( $4d^3-5s^1, 4d^{2.9}-5s^{1.1}, 4d^{2.8}-5s^{1.2}$ ). For Comparison between Free electron and Free atom, it is seen that in low momentum Free atom ( $4d^3-5s^1$ ) results higher than those the Free electron results ( $4d^3-5s^1$ ) but in part between  $p_z = (0.3$  and  $0.8)$  the trend reversed and the free electron values are somewhat larger than the free atom. At  $p_z > 0.9$

a.u. both models values become nearly similar. Fig. (2) shows the difference between theoretical (after convolution) and experimental profiles in Zr. It can be seen in the low momentum that  $\Delta J$  ( $4d^3-5s^1$ - Exp,  $4d^{2.9}-5s^{1.1}$  - Exp ,  $4d^{2.8}-5s^{1.2}$  - Exp) are larger than  $\Delta J$  ( $4d^{2.7}-5s^{1.3}$ -Exp), as well as the  $\Delta J$  (  $4d^{2.7}-5s^{1.3}$ -Exp), have similar values but different in low momentum, but (Free atom-Expt and Free Electron - Expt) are nearly the same where  $p_z > 1$  a.u. Also in the high momentum transfer region ( $p_z > 4$  a.u.), experimental values are very close to corresponding theoretical data. It is known that the contribution of valence electron is very small in this region and hence, most of the contribution may be due to the inner-core electrons. These inner-core electrons are reasonably described by the free-atom values. In order to determine the best configuration electrons, the total square deviation  $\sum_0^{7 a.u.} |\Delta J|^2$  was obtained

for each case .The values found were (0.2201599, 0 .2019151, 0 .1864189, 0 .1871129) for ( $4d^3-5s^1, 4d^{2.9}-5s^{1.1}, 4d^{2.8}-5s^{1.2}, 4d^{2.7}-5s^{1.3}$ ) configurations respectively. Therefor ( $4d^{2.8}-5s^{1.2}$ ) seems to be the best configuration. From this result we observe the effect of convolution on the theoretical values. The purpose of the computation of cohesion energy was to see the applicability of the RFA scheme in reproducing the cohesive of transition metals. The value of calculated cohesive energy (with  $p_{max}=2$  a.u.) is as in Table (2) that show comparison between theoretical results to cohesive energy by employing RFA model and another data. A choice of low value of  $p_{max}$  is justified because, to a good approximation, after this value the major contribution in the theoretical and experimental profile is expected only due to core electrons, which almost remain unaffected in formation of solids.

**Table(1): Theoretical values Compton profile of ( $\beta$ -Zr) compared with experimental valuey[24]. All the quantities are in atomic units , These values have been normalized to 16.60175 electrons .**

| $P_z$<br>(a.u.) | $J(p_z)(e/a.u.)$             |                                  |                             |                                     |                                     |                                     | Expt.<br>[24] |
|-----------------|------------------------------|----------------------------------|-----------------------------|-------------------------------------|-------------------------------------|-------------------------------------|---------------|
|                 | Free atom<br>( $4d^3-5s^1$ ) | Free electron<br>( $4d^3-5s^1$ ) | Theory(RFA)                 |                                     |                                     |                                     |               |
|                 |                              |                                  | Core<br>+RFA<br>$4d^3-5s^1$ | Core<br>+RFA<br>$4d^{2.9}-5s^{1.1}$ | Core<br>+RFA<br>$4d^{2.8}-5s^{1.2}$ | Core<br>+RFA<br>$4d^{2.7}-5s^{1.3}$ |               |
| 0.0             | 9.76                         | 7.945                            | 7.479                       | 7.439                               | 7.403                               | 7.365                               | 7.405         |
| 0.1             | 9.3                          | 7.896                            | 7.453                       | 7.415                               | 7.38                                | 7.343                               | 7.377         |
| 0.2             | 8.24                         | 7.741                            | 7.335                       | 7.304                               | 7.275                               | 7.243                               | 7.279         |
| 0.3             | 7.19                         | 7.479                            | 7.12                        | 7.102                               | 7.083                               | 7.06                                | 7.108         |
| 0.4             | 6.46                         | 7.092                            | 6.87                        | 6.864                               | 6.856                               | 6.841                               | 6.87          |
| 0.5             | 6.01                         | 6.58                             | 6.543                       | 6.552                               | 6.557                               | 6.553                               | 6.574         |
| 0.6             | 5.72                         | 5.941                            | 6.053                       | 6.064                               | 6.093                               | 6.11                                | 6.232         |
| 0.7             | 5.47                         | 5.174                            | 5.794                       | 5.78                                | 5.768                               | 5.752                               | 5.859         |
| 0.8             | 5.2                          | 4.836                            | 5.506                       | 5.494                               | 5.483                               | 5.469                               | 5.471         |
| 1.0             | 4.62                         | 4.79                             | 4.858                       | 4.849                               | 4.842                               | 4.832                               | 4.702         |
| 1.2             | 4.02                         | 4.16                             | 4.213                       | 4.209                               | 4.206                               | 4.2                                 | 4.016         |
| 1.4             | 3.49                         | 3.602                            | 3.635                       | 3.635                               | 3.635                               | 3.634                               | 3.457         |
| 1.6             | 3.06                         | 3.149                            | 3.161                       | 3.163                               | 3.166                               | 3.168                               | 3.029         |
| 1.8             | 2.73                         | 2.794                            | 2.792                       | 2.796                               | 2.801                               | 2.803                               | 2.704         |
| 2               | 2.48                         | 2.53                             | 2.524                       | 2.528                               | 2.533                               | 2.537                               | 2.461         |
| 3               | 1.85                         | 1.864                            | 1.857                       | 1.863                               | 1.869                               | 1.874                               | 1.803         |
| 4               | 1.44                         | 1.453                            | 1.445                       | 1.449                               | 1.454                               | 1.459                               | 1.433         |
| 5               | 1.08                         | 1.091                            | 1.083                       | 1.087                               | 1.09                                | 1.093                               | 1.081         |
| 6               | 0.807                        | 0.813                            | 0.807                       | 0.81                                | 0.813                               | 0.815                               | 0.803         |
| 7               | 0.613                        | 0.618                            | 0.613                       | 0.615                               | 0.617                               | 0.619                               | 0.607         |

**Table (2) : Cohesive energy of  $\beta$ -Zr.(  $E_{Coh}$ ( in eV))**

| Reference          | $E_{Coh}$ ( in eV) |
|--------------------|--------------------|
| Present work (RFA) | 6.67               |
| Experiment[25]     | 6.25               |

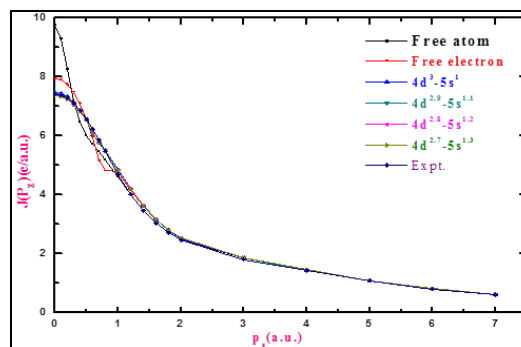


**Fig (1): Comparison of theoretical results with experimental Compton profiles [24] for  $\beta$ -Zr.**

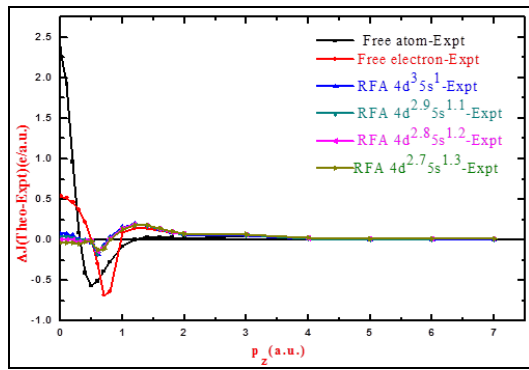


Fig (2): Difference between theoretical calculation and experimental Compton profiles [24]of  $\beta$ -Zr.

**b) Band structure and density of states:**

Figs.(3) and(4) show the energy bands and density of states of ( $\beta$ -Zr and  $\alpha$ -Zr) computed using LCAO-DFT-LDA scheme of quantum wise code in the energy range (-7 to 10) /eV for  $\beta$ -Zr and (-7.5 -10)/eV for  $\alpha$ -Zr. A few previous calculations of electronic structure of zirconium two phases have been reported

[25,26]. All results were obtained for the temperature 300°K. It is observed that the energy bands and density of states show characteristic features similar to ref [26], from Fig. (3-a and 4-a) there is an overlapping of valence and conduction bands confirming the 4d transition metal (Zr). It is seen in the present investigation the bands lying well below the Fermi level are due to 5s<sup>2</sup> electrons and the bands near the Fermi surface are due to 4d<sup>2</sup> electrons. The width of the conduction band decreases because of the enhanced overlap of the wave function with the neighboring atoms. Figs. (3-b,4-b) the density of state at the Fermi level is (0.2) eV for  $\alpha$ -Zr while this number was (1.5) eV for  $\beta$ -Zr. A nearly good agreement with other previous studies for example TB-LMTO, LAPW and FP-LMTO band structure calculations is observed. Figs. (3-a and 4-a) show energy bands in each k-points ( $\Gamma$ ,H,P,N) and ( $\Gamma$ ,M,L,A,K,H) for  $\beta$ -Zr and  $\alpha$ -Zr respectively.

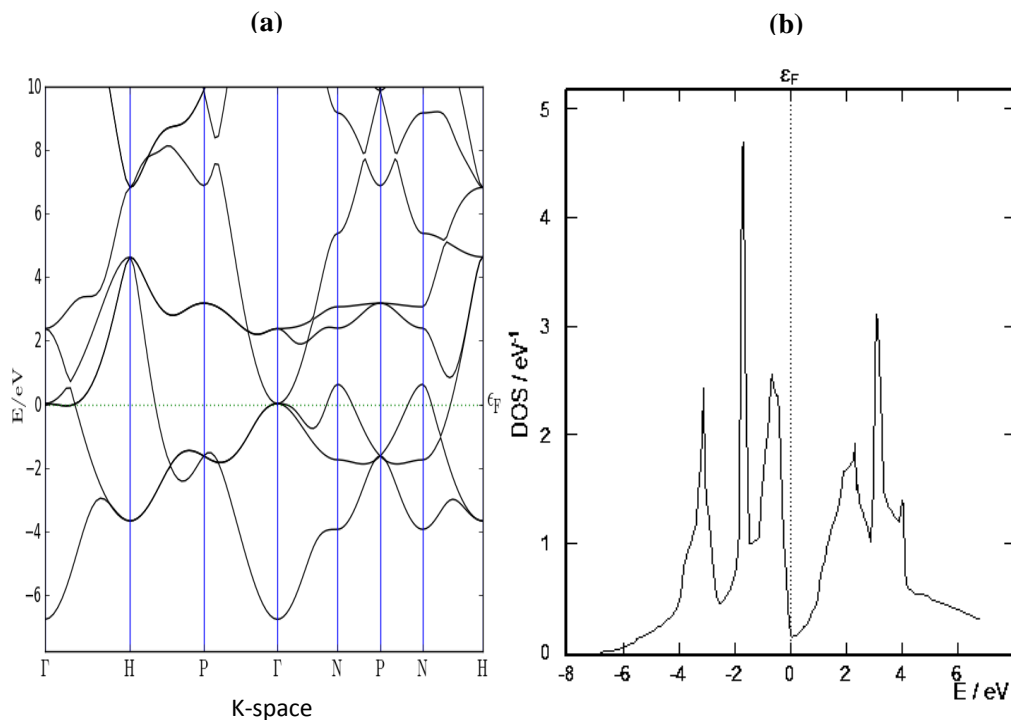
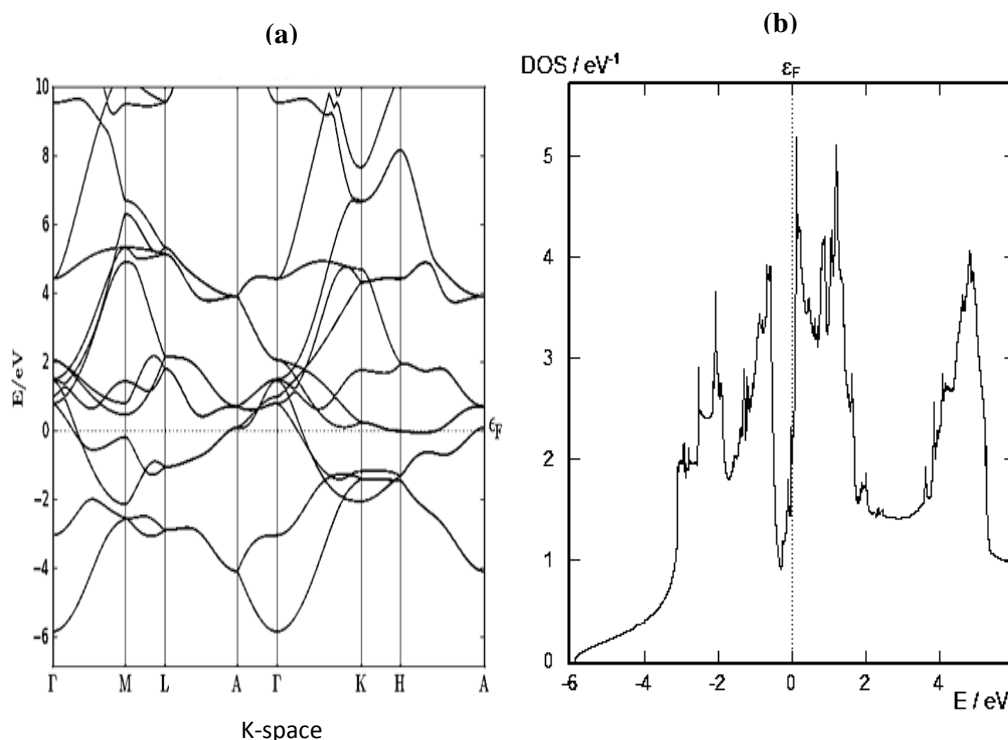


Fig (3-a,b): Band structure and total density of state of  $\beta$ -Zr along with high symmetry directions of the first BZ using LCAO (DFT-LDA).



**Fig (4-a,b): Band structure and total density of state of  $\alpha$ -Zr along with high symmetry directions of the first BZ using LCAO (DFT-LDA).**

#### 4. Conclusions

In present work theoretical calculations have been done using RFA model compared with experimental results [24]. The RFA model shows good agreement with the experiment in the ( $4d^{2.8}-5s^{1.2}$ ) configuration, but Compton profiles value using free electron model are higher than those obtained experimentally. Evidently, there is a need for a relativistic band structure calculation to interpret the Compton profile data. Table (1) illustrates the comparison between

#### Reference

- [1] C. Kittel" Introduction to solid state physics"5<sup>th</sup> edition, (Wiley Eastern) (1994).
- [2] S. L. Altmann and J. C. Bradley, Phys. Lett. 1, 336 (1962); Phys. Rev. 135A, 1253 (1964); Proc. R. Soc. 92, 769 (1967).
- [3] T. L. Loucks, Phys. Rev. 159, 544 (1967).
- [4] O. Jepsen, O. Krogh Andersen, and A. R. Mackintosh, Phys. Rev. B 12, 3084 (1975).
- [5] K. Iyakutti, C. K. Majumdar, R. S. Rao, and V. Devanathan, J. Phys. F 6, 1639 (1976).
- [6] P. Chatterjee, J. Phys. F 14, 2027 (1984).
- [7] Vaclev O. Kostroun, Robert W. Fairchild, Carl A. Kukkonen, and John W. Wilkins, Phys. Rev. B 13, 3268 (1976).
- [8] M. K. Harbola, R. R. Zope, A. Kshirsagar and R. K. Pathak, "Momentum-space properties from coordinate - space electron density", J. Chem. Phys., (2005), 122, 204110.
- [9] K.F. Berggren, S. Manninen, T. Paakkari, O. Aikala and K. Mansikka, Chapter *Solids* in a book

theoretical results using RFA model with previous work [24] in the process transfer charge of shells (s,d). The cohesive energy of  $\beta$ -Zr is computed by RFA model and compared with another results [25]. The energy bands and DOS computed by using the LCAO revealed metal character for  $\beta$ -Zr and  $\alpha$ -Zr respectively. Therefore, DFT -LDA calculations are sufficient to account the electronic properties of such materials .

entitled *Compton Scattering*, (Mc. Graw - Hill, London), pp. 139-209 (1977).

- [10] K.R.K. Ghandhi, and R.M. Singru, Philo. Mag. B 43,999 (1981).
- [11] B.L. Ahuja, B.K. Sharma, and O. Aikala, Pramana 29, 313(1987).
- [12] N.I. Papanicolaou, N.C. Bacalis and D.A. Papaconstantopoulos. Phys. Rev. B 37,862(1988).
- [13] N.G. Alexandropoulos, S.K. Danakas, K.T. Kotris and N. I. Papanicolaou . Solid State Comm.92, 453 (1985).
- [14] L.Y-Shou ,L. A. Yu and Z.Z. Zhong .Chinese Physics Letters Volume 21.No 9.PP 1791-1795 (2004).
- [15] M. J. Cooper, P. E. Mijnarends, N. Shiotani, N. Sakai, and A. Bansil." X-ray Compton Scattering", volume 5 of Oxford Series on Synchrotron radiation. Oxford University Press, (2004).
- [16] K.F. Berggren, Phys .Rev.B6.2156 (1972).
- [17] K.F. Berggren, S. Manninen, and T. Paakkari , Phys. Rev. B552516(1973).

- [18] B.K Sharma., A Gupta., H Singh., S. Perkkiö., A Kshirsagar. and D.G. Kanhere. Phys. Rev B37 6821 (1988).
- [19] L. Biggs, L. Mendelsohn, J.B. Band Mann , At Data Nucl. Data Table 16,201(1975).
- [20] R.S. Holt, M.J. Cooper," The calculation of electronic energies from Compton profiles". Philos. Mag. B 41(2), 117-121,(1980).
- [21] R.G. Parr and W. Yang "Density Functional Theory of Atoms and Molecules" University press, New York(1989).
- [22] W. Kohn and L.J. Sham, Phys. Rev. 140, A1133(1965).
- [23] K. Stokbro, D. E. Petersen, S. Smidstrup, A. Blom, M. Ipsen and K. Kaasbjerg, Phys. Rev. B 82,075420 (2010).
- [24] B. K. Sharma and B. L. Abuja Phys. Rev. B ,vol 38,N 5 (1988).
- [25] Z. Wei, D. Singh, and H. Krakauer . Phys. Rev B, Vol 36.No14 ,(1987).
- [26] G. Jency and S. Kumari. Univeral Journal of Chemistry 1(2):pp 64-70,(2013).

## دراسة التركيب الإلكتروني للغلافين (s-d) لعنصر الزركونيوم ذي طور بيتا

عبد الهادي مردان غالب

قسم الفيزياء ، كلية العلوم ، جامعة كركوك ، كركوك ، العراق

### الملخص

البحث يتضمن حساب منحني كومبتن لطور بيتا لعنصر الزركونيوم باستخدام النموذجين (اعادة المعايرة الحرة والكترون الحر) لمختلف الترتيبات الكترونية ( $4d^{3-x}-5s^{1+x}$ ) حيث ان ( $x=0$  to 1 step 0.1), تم حصول على توافق جيد بين البيانات النظرية والعملية المأخوذة من احدى المصادر المشار اليه في متن البحث ,وان افضل ترتيب الكتروني وجد عند ( $4d^{2.8}5s^{1.2}$ ). وكذلك حسبت طاقة التماسك من النتائج النظرية وقورنت مع البيانات السابقة. اوجد التركيب الحزمي وكثافة الحالات لطورين (بيتا والفا) لعنصر الزركونيوم ضمن نظرية الدالي للكثافات باستعمال شفرة (Quantum wise-ATK) وباستخدام طريقة تقريب كثافة الموضع.

**الكلمات المفتاحية:** منحني كومبتن , نموذج اعادة المعايرة الحرة , نموذج الكترون الحر , شفرة (Quantum wise-ATK), طاقة التماسك.